Supplementary Material

Supplementary Figure 1. A large fast, continuous spiking parvalbumin immuno-positive interneurone in layer 4 of cat visual cortex elicits a fast IPSP in a layer 4 pyramidal cell.
In A the IPSP elicited in the pyramidal cell is illustrated. B. The continuous firing of this interneurone in response to a suprathreshold current pulse is shown in B. In C the reconstruction of this interneurone (dendrites red, axon blue) and the postsynaptic pyramid (dendrites black) is shown. The dendrites of this interneurone extend into layers 3 and 5, suggesting that this cell receives input in 3 layers, but its broad axonal arbour is largely confined to the layer of origin, layer 4. At higher magnification (D) points of close membrane apposition between the interneuronal axon and a primary, a secondary and a tertiary pyramidal dendrite (blue circles) and between the interneuronal axon and its parent dendrites (blue squares, putative autapses) are illustrated. In E Immuno-fluorescent labelling of this slice demonstrates that this interneurone is immuno-positive for parvalbumin (green) and immuno-negative for calbindin (red).

Supplementary Figure 2. A strongly adapting/burst firing parvalbumin immuno-negative double bouquet interneurone in layer 4 of cat visual cortex elicits IPSPs in two postsynaptic layer 4 pyramidal cells.
In A the reconstruction of this interneurone (dendrites red, axon blue) and two postsynaptic pyramids (dendrites black and green respectively) is shown. The dendrites of this interneurone are confined to the layer of origin, layer 4, but narrow projections of its axonal arbour extend up to layer 1 and down into layer 6. Averaged IPSPs elicited by single presynaptic APs are shown in B for both postsynaptic cells. Note that the green cell which is on the outskirts of the interneuronal axonal arbour, received a slower IPSP (half width 29ms) than the black cell (half width 14.2ms) which is closer to its centre. Averaged IPSPs recorded at 3 membrane potentials (black pyramid) are shown. The averaged IPSP recorded at -60mV is superimposed on the IPSP recorded at -50mV demonstrating that a small decrease in duration is associated with more hyperpolarized membrane potentials. The extrapolated reversal potential was -67mV. Depression of this IPSP is apparent in C which shows responses to pairs and triplets of interneuronal Aps.

Supplementary Figure 3 . A narrow spike, stopping/stuttering multipolar interneurone in layer 4 of cat visual cortex elicits fast IPSPs in a postsynaptic layer 5 pyramidal cell.
In A the reconstruction of this interneurone (dendrites red, axon blue) is shown. Dotted lines in the axonal reconstruction indicate myelinated portions. The position of the soma of the postsynaptic pyramid (not reconstructed) is indicated by the grey triangle. The dendrites of this interneurone are confined to the layer of origin, layer 4. Its axon extends horizontally within layer 4 and vertically down into layer 6. Averaged IPSPs (half width 8ms) elicited by brief spike pairs and recorded at 3 membrane potentials are shown in B. Extrapolated reversal potential -73mV. Strong paired pulse depression of this IPSP is apparent. In C the continuous non-accommodating firing that can be elicited in this interneurone with suprathreshold depolarization is shown.

Supplementary Figure 4. A large, narrow spike, stopping/stuttering multipolar interneurone in layer 4 of cat visual cortex elicits large, fast IPSPs in a postsynaptic layer 4 spiny stellate cell.
This interneurone was identified and had an axonal arbour whose distribution resembled that in Figure 4, but was only partially recovered and not reconstructed. The IPSP elicited at 4 postsynaptic membrane potentials is shown in A (half width 7.8ms) and the plot used to estimate the reversal potential (-68mV) in B. Averaged IPSPs elicited by brief spike pairs and recorded at -43mV are shown in C. Again, paired pulse IPSP depression is apparent. In D and F, powerful depression during longer trains of presynaptic APs is illustrated.

Supplementary Figure 5. A slow spiking, stopping/stuttering bipolar interneurone in layer 4 of cat visual cortex elicits is reciprocally connected to a postsynaptic layer 4 pyramidal cell.
This interneurone was identified and had a dense local axonal arbour, but was only partially recovered and not reconstructed. Both the EPSP elicited by the presynaptic pyramid (A) and the IPSP in the pyramidal cell (B) demonstrate depression. Interactions between these two cells when both are close to firing threshold are shown in C and D. In C, the train of IPSPs (top black trace) elicited in the pyramid by an interneuronal spike train (top red trace) can be seen to slow pyramidal firing (middle black trace) when compared with the lower black traces recorded when the interneurone did not fire (lower red trace). D With a just suprathreshold pulse the interneurone fires consistently at the start of the pulse, but only twice, in a stuttering fashion in response to each pulse (top red trace). When the pyramidal cell is triggered to fire concomitantly (lower black trace), the two cells synchronize, with the interneurone firing more consistently and typically twice as fast as the pyramidal cell.

Supplementary Figure 6. Evidence for a presynaptic locus for synaptic facilitation and depression and correlations with EPSP time course.
In **a**. the normalised inverse square of the coefficient of variation ($CV^{-2} = np/1-p$) is plotted against the normalised mean EPSP amplitude ($M = npq$) for adult rat ($n = 7$, closed symbols) and cat (open circles $n = 6$) connections. Second and third EPSPs at different interspike intervals are included and their mean amplitudes and coefficients of variation normalised to those of the 1st EPSP. The majority of the points fall on slopes >1 suggesting that both facilitation and depression are mediated predominantly presynaptically and by a change in the probability of release (p) and/or in the number of release sites contributing to the EPSP (n) and not by a change in the quantal amplitude (q). In **b**. the paired pulse ratio (2nd EPSP as a % of the 1st EPSP average amplitude) is plotted against the percentage of 1st EPSPs that appeared to be total failures of transmission (6 cat, 7 adult rat and 18 juvenile rat connections in which sufficient failures were recorded). This demonstrates that the failure rate is consistently higher in connections that subsequently display facilitation. The dotted lines are included to indicate the approximate limits of connections that facilitate and depress respectively. In **c.** (adult) and **d.** (juvenile) paired pulse ratio is plotted against EPSP 10-90% rise time and in **e.** and **f.** paired pulse ratio is plotted against EPSP width at half amplitude. The vertical dotted lines indicate the maximum rise times and half widths associated with narrow spike interneurones and the horizontal lines mark paired pulse ratios of 100%. For the adult connections the symbols indicate the interspike intervals at which the measurements were made: open circles 5ms, filled circles 10ms, open squares 20ms and filled triangles 50ms. All measurements in juveniles were made at an interspike interval of 50ms. These relations, unlike that shown in Figure 8. where paired pulse ratio is plotted against the width of the AP at half amplitude, are far from linear, but indicate a population of fast, depressing connections and a population of broader facilitating EPSPs, with perhaps an intermediate duration population that also depress.

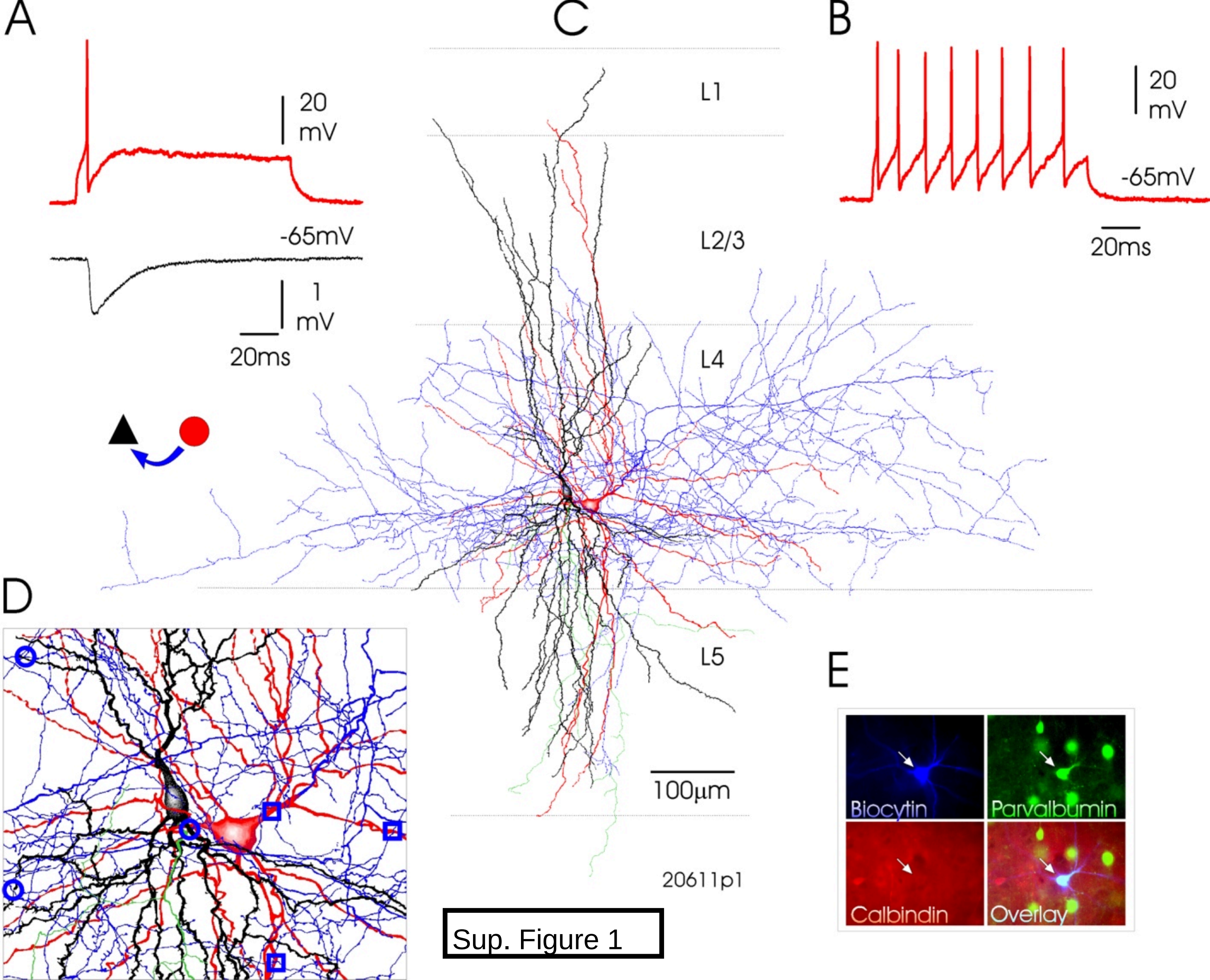
A
20 mV
-65mV
1 mV
20ms
C
L1
L2/3
L4
L5
100µm
20611p1
B
20 mV
-65mV
20ms
D
E
Biocytin
Parvalbumin
Calbindin
Overlay

Sup. Figure 1

A

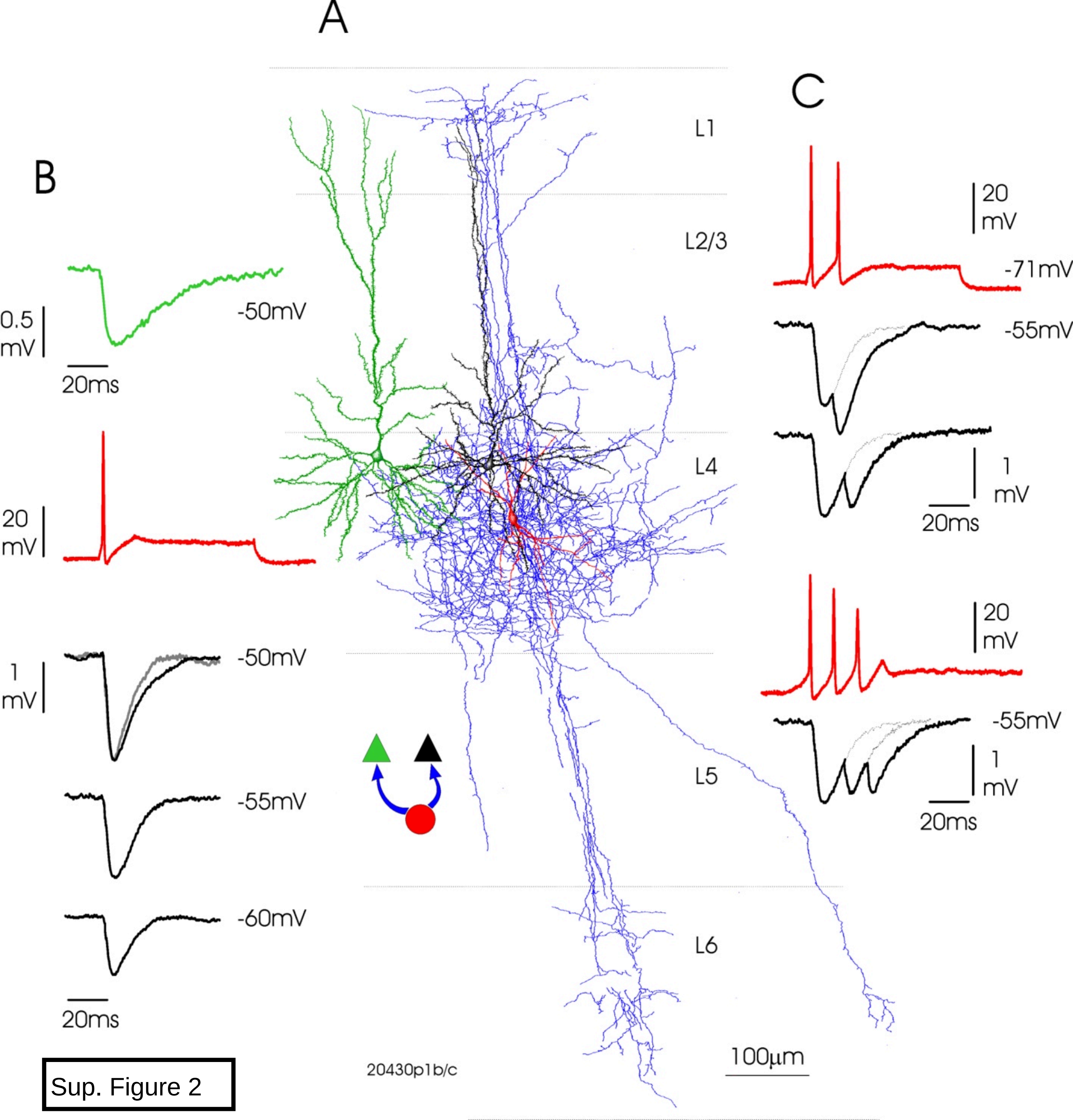

Sup. Figure 2

Sup. Figure 3

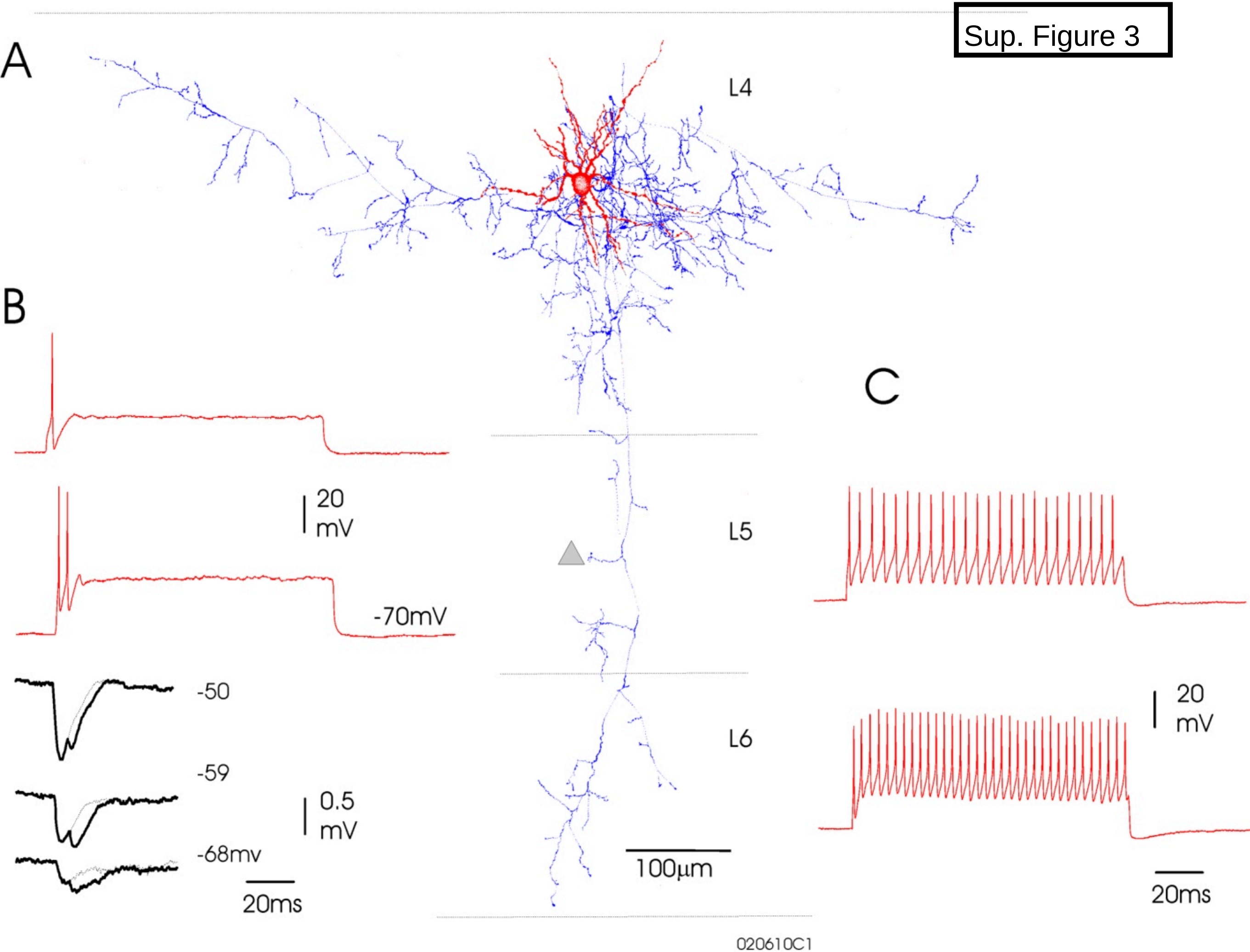
A
L4
L5
L6
100µm
020610C1
B
20
mV
-70mV
-50
-59
-68mv
0.5
mV
20ms
C
20
mV
20ms

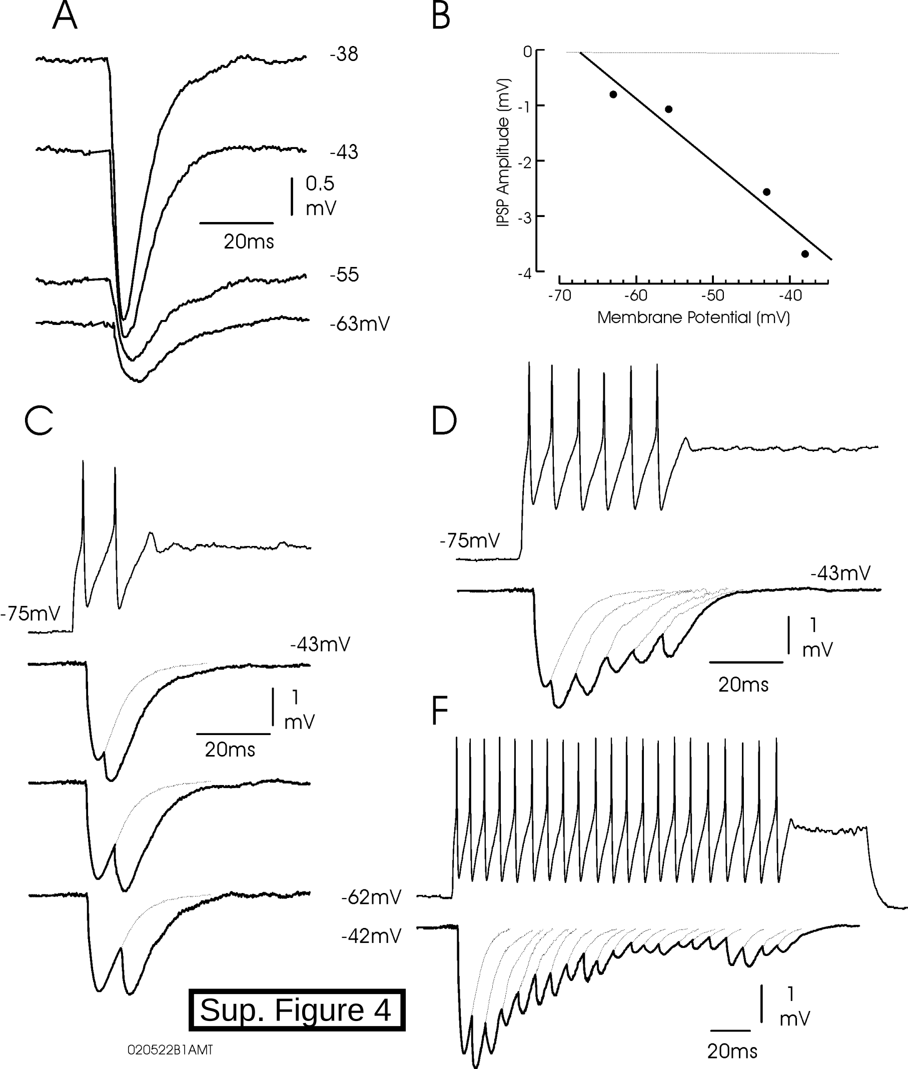

Sup. Figure 4

020522B1AMT

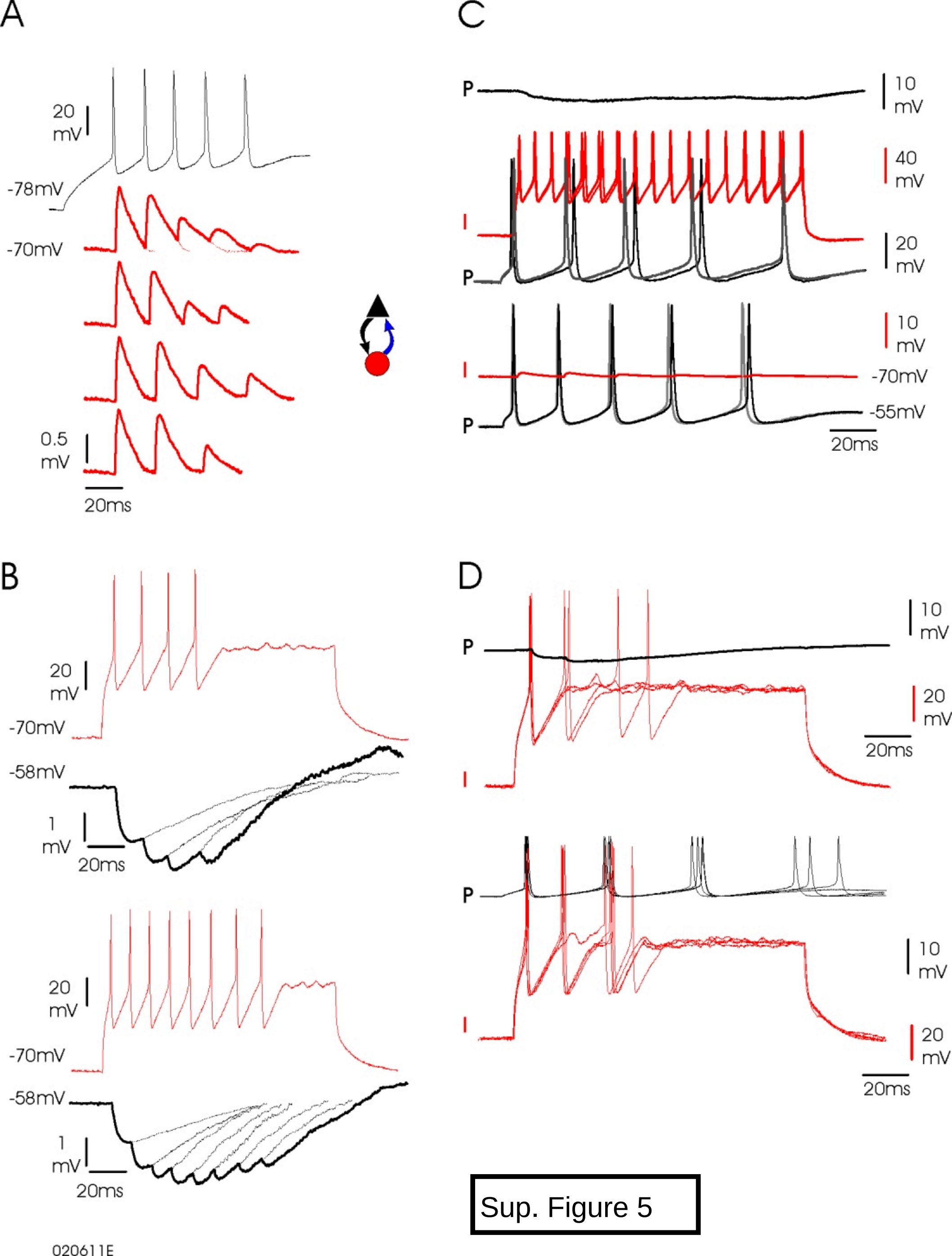
A
20
mV
-78mV
-70mV
0.5
mV
20ms
B
20
mV
-70mV
-58mV
1
mV
20ms
20
mV
-70mV
-58mV
1
mV
20ms
020611E
C
P
10
mV
40
mV
I
20
mV
P
10
mV
I
-70mV
P
-55mV
20ms
D
P
10
mV
20
mV
20ms
I
P
10
mV
I
20
mV
20ms

Sup. Figure 5

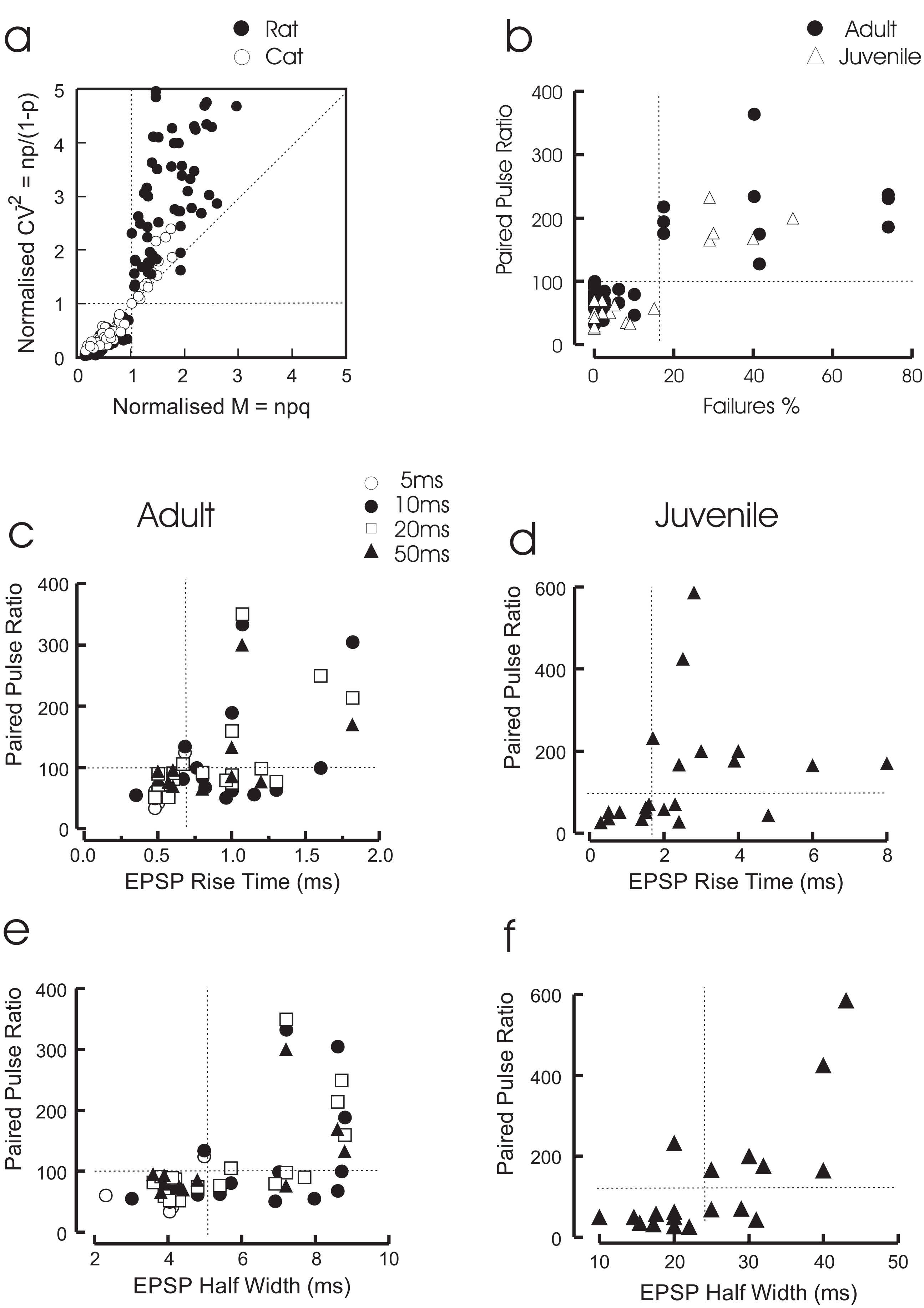

Supplementary Figure 6.